Peptides GWN and GW protect kidney cells against Dasatinib induced mitochondrial injury in a SIRT1 dependent manner

Khushwant S. Bhullar [a,b], Fatemeh Ashkar [a], Jianping Wu [a,*]

[a] *Department of Agricultural, Food, and Nutritional Science, University of Alberta, Edmonton, AB, Canada*
[b] *Department of Pharmacology, University of Alberta, Edmonton, AB, Canada*

ARTICLE INFO

ABSTRACT

Dasatinib, a small-molecule drug used as a treatment for chronic myeloid leukemia induces mitochondrial damage in embryonic kidney (293 T) cells ($p < 0.05$). This dasatinib induced mitochondrial injury in kidney cells was mitigated by H3K36me3 activating ovotransferrin-derived peptides GWN and GW. Pre-treatment of kidney cells with GWN and GW lead to elevation of cytoprotective sirtuins, SIRT1 and SIRT3, in response to dasatinib injury ($p < 0.01$) *in vitro*. Both peptides, GWN and GW, also reversed dasatinib induced the loss of mitochondria in kidney cells and promoted the protein expression of COX4 ($p < 0.01$). Mechanistically, loss of SIRT1 in kidney cells abolished the ability of GWN and GW to protect embryonic kidney cells against dasatinib injury *in vitro*. Overall, we provide cell based evidence showing that GWN and GW exhibit the ability to protect mitochondria against dasatinib-induced mitochondrial damage in a SIRT1 dependent manner.

1. Introduction

Mitochondria are quintessential eukaryotic organelles of proteo-bacterial origin that perform a wide range of core cellular processes (Martijn, Vosseberg, Guy, Offre, & Ettema, 2018). Renowned as the powerhouses of the cell, mitochondria perform multiple metabolic functions and regulate the key processes of apoptosis, cancer, and aging (Burke, 2017; Spinelli & Haigis, 2018). Among the physiological roles of mitochondria, the maintenance of redox homeostasis is a vital function, as mitochondria are the important sources of free radicals such as superoxide ion ($O_2^{\bullet-}$), hydrogen peroxide (H_2O_2), and peroxyl radical ($OH^\bullet$) (Kluge, Fetterman, & Vita, 2013). Accelerated production of these oxidant species can lead to redox imbalance or oxidative stress, which may instigate physiological dysfunction in vital organs (Kluge et al., 2013; Sena, Pereira, & Seiça, 2013). Kidneys are second only to the heart in the mitochondrial count and key oxygen utilizers, thus a major target of oxidative stress (Hoenig & Zeidel, 2014). The presence of abundant long-chain polyunsaturated fatty acids in the composition of renal lipids makes kidneys extensively vulnerable to free radical damage (Balat, Resic, Bellinghieri, & Anarat, 2012; Krata, Zagożdżon, Foroncewicz, & Mucha, 2018). Apart from intrinsic cellular oxidative stress, extrinsic nephrotoxicity induced by chemotherapy is also a major source of oxidative damage in kidneys (Piscitani, Sirolli, Di Liberato, Morroni, & Bonomini, 2020).

One of the inducers of oxidative stress in kidneys is dasatinib, a drug used for the treatment of leukemia(s) (Piscitani et al., 2020; Xue et al., 2012). Various clinical case reports have testified kidney damage and failure caused by dasatinib (Holstein, Stokes, & Hohl, 2009; Ozkurt, Temiz, Acikalin, & Soydan, 2010; Wallace, Lyndon, Chumley, Jaimes, & Fatima, 2013). Additionally, dasatinib has also been shown to drastically induce mitochondrial damage and oxidative stress in cells leading to apoptosis (Bouitbir, Panajatovic, Frechard, Roos, & Krähenbühl, 2020; Guignabert et al., 2016; Xue et al., 2012). Thus, alleviating oxidative stress is a viable strategy for reducing dasatinib-induced mitochondrial damage, particularly in susceptible vital organs like kidneys. One of the potential cytoprotective signal(s) which can help in the alleviation of oxidative damage caused by dasatinib is histone 3 tri-methylation at lysine 36 (H3K36me3) (Sun et al., 2020). H3K36 residue participates in genomic stability and transcription and is found in various methylated forms (DiFiore, Ptacek, Wang, Li, Simon, & Strahl, 2020). The early clues about H3K36me3 induced cytoprotection came from yeast and were later explored in other model systems as well (Tu et al., 2007). Consistent with the studies in yeast, studies in mammals, found H3K36me3 being tightly associated with active transcription and DNA protection (Sims Iii & Reinberg, 2009). Later studies showed that global downregulation of H3K36me3 leads to diminished overall cell

---

survival (Cermakova, Smith, Veverka, & Hodges, 2019). Further, this pattern of histone modifications might also be influenced by SIRT1, a vital histone deacetylase, involved in cell survival, and alleviation of oxidative damage (Li et al., 2020). Given the importance of H3K36me3, identification of cytoprotective small molecules with the ability to modulate this histone mark depending on physiological petitions to counter oxidative stress is a rational approach.

One group of small molecules which have gained attention as potent antioxidants and cytoprotective molecules are bioactive peptides (Bhullar & Wu, 2020). Owing to their ability to boost mitochondrial antioxidant enzymes and improve overall metabolic health, they hold a strong potential in the alleviation of dasatinib-induced mitochondrial stress (Bhullar et al., 2021a; Fan, Bhullar, & Wu, 2021). Also, the lack of any significant effect on the oral bioavailability of dasatinib in presence of antioxidant nutraceuticals supports the exploration of detoxifying antioxidant peptides (Maher, Alzoman, Shehata, & Abanmy, 2018). An abundant source of antioxidant peptides to counter oxidative damage and cytotoxicity is ovotransferrin, a major protein in egg white (Lee, Moon, Kim, Park, Ahn, & Paik, 2017; Shang, Bhullar, & Wu, 2020). Our group has identified multiple antioxidant and cytoprotective peptides from ovotransferrin with a spectrum of pharmacological properties (Jahandideh, Chakrabarti, Davidge, & Wu, 2016; Shen, Chahal, Majumder, You, & Wu, 2010). In one of our reports, we identified two new peptides, GWN and GW, from ovotransferrin with strong antioxidant activity (Jahandideh et al., 2016). Among these, GW diminished TNFα-induced VCAM-1 expression in human umbilical vein endothelial cells (HUVECs), a recognized model system for investigating oxidative and mitochondrial damage (Jahandideh et al., 2016; Wu, Wang, & Nabi, 2019). As dasatinib induces substantial oxidative damage and decline in mitochondrial cytochrome *c* oxidase subunit 4 (COX4) activity (Will et al., 2008), we hypothesize that peptides GWNI, GWN, and GW, owing to their antioxidant activity may protect kidney cell mitochondria against dasatinib injury, possibly via H3K36me3 and/or SIRT1 pathway.

2. Materials and methods

2.1. Chemicals and reagents

Dasatinib (SML2589) was purchased from Millipore-Sigma (Oakville, ON, Canada). RIPA buffer was obtained from Abcam (Toronto, ON, Canada). Halt protease and phosphatase inhibitor single-use cocktail (100X) was obtained from Life Technologies Inc. (Burlington, ON, Canada). VWR disposable pestle was obtained from VWR International (Mississauga, ON, Canada). DMEM, FBS, Penicillin-Streptomycin solution, HEPES buffer, EDTA-trypsin, and nuclease-free water were obtained from Life Technologies Inc. (Burlington, ON, Canada). SIRT1 (ab189494), COX4 (ab197658), TFAM (ab272885), Catalase (ab223793), SOD2 (ab13534), and GAPDH (ab8245) were obtained from Abcam (Toronto, ON, Canada). Tri-methyl-Histone H3 (Lys36) rabbit pAb (H3K36me3, PTM-625) was obtained from PTM Bio LLC (Chicago, IL, USA).

2.2. Cell culture

293 T cells (CRL-3216™) were purchased from American Type Culture Collection (ATCC, Manassas, VA, USA). The 293 T cells were cultured in 100x15mm Nunc™ cell culture dishes (Thermo Fisher Scientific, ON, Canada) at initial density of 50,000 cells per plate. The cells were maintained in Dulbecco's Modified Eagle's Medium (DMEM) supplemented with 10% fetal bovine serum (FBS) and 1% Penicillin-Streptomycin at 37 °C with 5% CO_2. The cells were cultured for the indicated times and observed using a microscope until they reached ∼ 70 % confluence. Upon reaching this confluency level, the cells were treated with dasatinib (1 μM) or the selected peptides (50 μM).

2.3. Peptide synthesis

The three ovotransferrin-derived peptides, GWNI GWN, and GW were synthesized by GenScript (Piscataway, NJ, USA). Peptide sequence and purity (99.8%) were validated by high-performance liquid chromatography − tandem mass spectrometry (HPLC-MS/MS). The peptides were reconstituted in water (100 mM stock), and their aliquots were stored at −20 °C until further experiments.

2.4. Cell treatment

Embryonic kidney cells (293 T) were cultured as described above and were treated with either dasatinib or peptides after reaching ∼ 70% confluence. This confluency level was chosen to give the ample time for cells to reach full confluency in presence of the pharmacologically active peptides. Briefly, to check the ability of dasatinib to induce mitochondrial-DNA damage, 1 μM dasatinib was added for 6 h. Next, to investigate the cytoprotective abilities of candidate peptides, kidney cells were pre-incubated for 24 h with peptides, followed by cellular stress of dasatinib (1 μM). Following these treatments, protein, histones and trypsinized cells were obtained. The dose selection of peptides was based on our previous report indicating the efficacious dose of 50 μM (Jahandideh et al., 2016) while dasatinib dose selection (1 μM) was based on its IC_{50} value in cancer cell lines ($IC_{50} < 1$ μM) (Tryfonopoulos, O'Donovan, Corkery, Clynes, & Crown, 2009).

2.5. Cell viability

Cell viability was assessed using TC10™ Cell Counter (Biorad, Mississauga, ON, Canada). Following treatment with peptidesf, GWNI GWN, and GW, 293 T cells were trypsinized, washed twice with PBS, and resuspended in complete media after centrifugation. The cell viability was assessed using the trypan blue method on dual-chamber cell counting slides for TC10™ Cell Counter (Biorad, Mississauga, ON, Canada).

2.6. Protein and histone extraction

Protein was extracted from the cells using RIPA buffer supplemented with protease inhibitors. After treatment, media was removed from culture plates, and cells were washed twice with 10 mL ice-cold PBS. After washing, 300 μL of RIPA Lysis buffer with protease inhibitors was added to 10 cm plate, and cells were scraped using a cell scraper. The cell lysate was incubated on ice for 15 min and then further lysed manually with a disposable pestle. Next, the lysate was incubated for additional 15 min and centrifuge at 13,000 × g for 5 min at 4 °C to collect protein supernatant. The pellet was used to extract histones according to a previously described method (Shechter, Dormann, Allis, & Hake, 2007). After the total protein extraction as described above, acid-based precipitation of histones was conducted as described earlier (Shechter et al., 2007). The pH of extracted histones was neutralized using 0.5 M NaOH (1:1 v/v) before immunoblotting.

2.7. Western blot

Following treatment with the vehicle, dasatinib, and/or candidate peptides, the culture medium was removed, and the cells were lysed using RIPA buffer as described in the previous section. These cell lysates were run on SDS-PAGE, transferred to nitrocellulose membranes, and immunoblotted with primary antibodies according to the recommended concentration(s) by manufacturer. After incubating with the secondary antibodies, protein bands were detected using a Licor Odyssey Bio-Imager (Licor Biosciences, Lincoln, NB) and quantified by densitometry using Image Studio Lite 5.2 software, as described in our recent report (Bhullar et al., 2021a).

2.8. Flow cytometry

Flow cytometry was performed at the University of Alberta's flow cytometry core facility. The content or density of mitochondrial in cells was measured by the MitoTracker™ Green FM (Invitrogen™, M7514) based on the manufacturer's instructions using a flow cytometer (FACS Canto II, BD Bioscience, CA, USA). Briefly, cells were cultured and treated as indicated above. After treatment, cells were trypsinized, collected, and resuspended in buffer made from PBS and FBS (3:1) with MitoTracker™ Green FM at 400 nM concentration. After incubation with dye for 45 min at 37 °C, mitochondrial content was analyzed using the BD FACSCanto™ (BD FACS Canto II) flow cytometry cell analyzer (BD Biosciences, San Jose, CAL, USA). The FlowJo software was used for the analysis of flow cytometry data (Tree Star, Inc. OR, USA).

2.9. DNA extraction and agarose gel

First, the mitochondria were extracted from the cells as per our recent report (Bhullar et al., 2021a). Next, according to a previous report, DNA extraction was conducted (Boccellino et al., 2003). Briefly, cells from 10 cm plate were re-suspended in 500 µL Tris–EDTA buffer and lysed with 0.2% Triton X-100. In the presence of 0.5 M NaCl, DNA was precipitated in ethanol for 6 h. Then, high-speed centrifugation was employed for DNA sedimentation, and the fragmented DNA extract from the aqueous phase was precipitated with isopropanol. The samples were incubated with RNase A (0.1 mg/mL) for 30 min at 37 °C after Tris–EDTA buffer resuspension. Finally, the extracted DNA was run on a agarose gel with SYBR™ Safe DNA gel stain stain.

2.10. KO cells

293 T SIRT1 KO cells were prepared using the CRISPR-Cas9 methodology described in our recent report (Bhullar et al., 2021b). The oligonucleotide sequences included SIRT1 crRNA: CUGAAUAUACCU-CAGCGCCA, SIRT1 Sequencing Primer Fwd: TTTTCA-CACTTCCCTCCTTCAT, SIRT1 Sequencing Primer Rev: TCCTTGCTCTATCGAGTTCACA. The KO cells were treated with dasatinib (1 µM) and/or peptides (50 µM) as described in the sections above.

2.11. ROS and antioxidant enzyme measurement

Reactive oxygen species (ROS) were measured in cells using a ROS assay kit obtained from Abcam (Toronto, ON, Canada). The kit uses cell permeant reagent $2',7'$ –dichlorofluorescin diacetate (DCFDA) to quantitatively assess ROS in live cell samples, which can be detected by fluorescence spectroscopy with excitation/emission at 485 nm/535 nm. For ROS measurement, cells were seeded at density of 25,000 cells per well in a 96 well plate black bottom plates. All the steps were carried out as per instructions given in the supplier's protocol for adherent cells (ab113851). The protein levels of antioxidant enzymes, SOD2, and Catalase, were measured using cell treatment (as in section 2.4) and western blot analysis.

2.12. Metabolism prediction

Metabolism prediction was conducted by SwissADME and detailed metabolic parameters were evaluated separately by software methods. Key parameters such as topological polar surface area (TPSA); iLOGP (for implicit log P) based on Gibbs free energy of solvation calculated by GB/SA in water and n-octanol; log Kp (with Kp in cm/s), the skin permeability index; bioavailability score, the probability of a compound to have at least 10% oral bioavailability in the rat model; along with GI and brain absorption were calculated. Briefly, the canonical smiles of the two active peptides, GWN and GW, were generated using Open Babel software. The strings of two peptides, NCC(=O)N[C@@]([H])(CC (=CN2)C1 = C2C = CC = C1)C(=O)N[C@@]([H])(CC(=O)N)C(=O)O and NCC(=O)N[C@@]([H])(CC(=CN2)C1 = C2C = CC = C1)C(=O)O, were fed to the SwissADME along with known drug molecules Ibuprofen {CC(C)CC1 = CC = C(C = C1)C(C)C(=O)O} and Omeprazole {CC1 = CN = C(C(=C1OC)C)CS(=O)C2 = NC3 = C(N2)C = CC(=C3)OC}. The program was run to obtain the BOILED-Egg results while the pharmacological data was obtained using CSV file provided by SwissADME.

2.13. Statistical analysis

All data are presented as mean ± standard deviation (SD) of a minimum of three independent experiments. All statistical analyses were performed using GraphPad Prism software version 5.02 (GraphPad Software, San Diego, CA, USA). Data were analyzed using one-way analysis of variance (ANOVA) followed by Dunnett's post-hoc test (w. r.t vehicle). $P < 0.05$ was considered significant.

3. Results

3.1. Impact of dasatinib on kidney cells

Firstly, mitochondria damage was induced using dasatinib (1 µM) in 293 T embryonic kidney cells (Fig. 1A). Next, the mitochondria were extracted, and the DNA gel analysis showed that the dasatinib exposure leads to significant mt.DNA fragmentation (Fig. 1A). The DNA fragmentation induced by dasatinib was significantly higher than the vehicle used throughout this study (DMSO). Further, the treatment of kidney cells with dasatinib (1 µM) also resulted in a significant decrease in the protein levels of COX4 ($p < 0.05$) compared to the vehicle group in the extracted mitochondria (Fig. 1B). These two experiments confirmed the establishment of mitochondrial damage induced by dasatinib in kidney cells *in vitro*.

3.2. Toxicity and histone analysis of ovotransferrin peptides

A comparative *in vitro* toxicology study was conducted to assess the impact of ovotransferrin peptides (GWNI, GWN, and GW) on 293 T cells *in vitro* (Fig. 2A). The trypan blue viability analysis showed that all the tested peptides (GWNI, GWN, and GW) exhibited > 90% cell viability in human embryonic kidney cells (Fig. 2B). However, among these peptides, GWNI showed statistically significant cytotoxicity ($p < 0.05$), indicated by a decline in cell viability, while GW and GWN maintained the highest cell viability and exhibited low toxicity *in vitro* (Fig. 2B). We also tested the effect of the three peptides (GWNI, GWN, and GW) for their ability to induce cytoprotective histone modification, H3K36me3, in kidney cells (Fig. 2C). Among GWNI, GWN, and GW, GWN and GW (50 µM) resulted in a significant accumulation of active histone mark H3K36me3 ($p < 0.05$ and $p < 0.01$ respectively), suggesting a potent cytoprotective ability of GW and GWN peptides on cellular oxidative stress and DNA damage. However, GWNI treatment (50 µM) did not enhance the cytoprotective active histone mark H3K36me3 compared with the vehicle group (Fig. 2C). These experiments established a safe toxicological and cytoprotective profile of GWN and GW, with the exclusion of GWNI from a further set of experiments. Although it is vital to note that GWNI treatment did exhibit > 90% viability, highlighting an acceptable safety profile but statistical analysis was taken into consideration for its exclusion from further set of experiments.

3.3. Cytoprotective ability of GWN and GW against dasatinib stress

First, we evaluated the ability of two ovotransferrin derived peptides, GWN and GW, against dasatinib induced cellular injury (Fig. 3A). It has been reported that SIRT1, an NAD$^+$ dependent protein deacetylase, regulates the cellular stress response. Pre-treatment of kidney cells with GWN and GW (50 µM), countered dasatinib stress via a significant increase in the protein level of SIRT1 in 293 T cells ($p < 0.01$) (Fig. 3B). Our results also showed that GWN (50 µM), but not GW, significantly
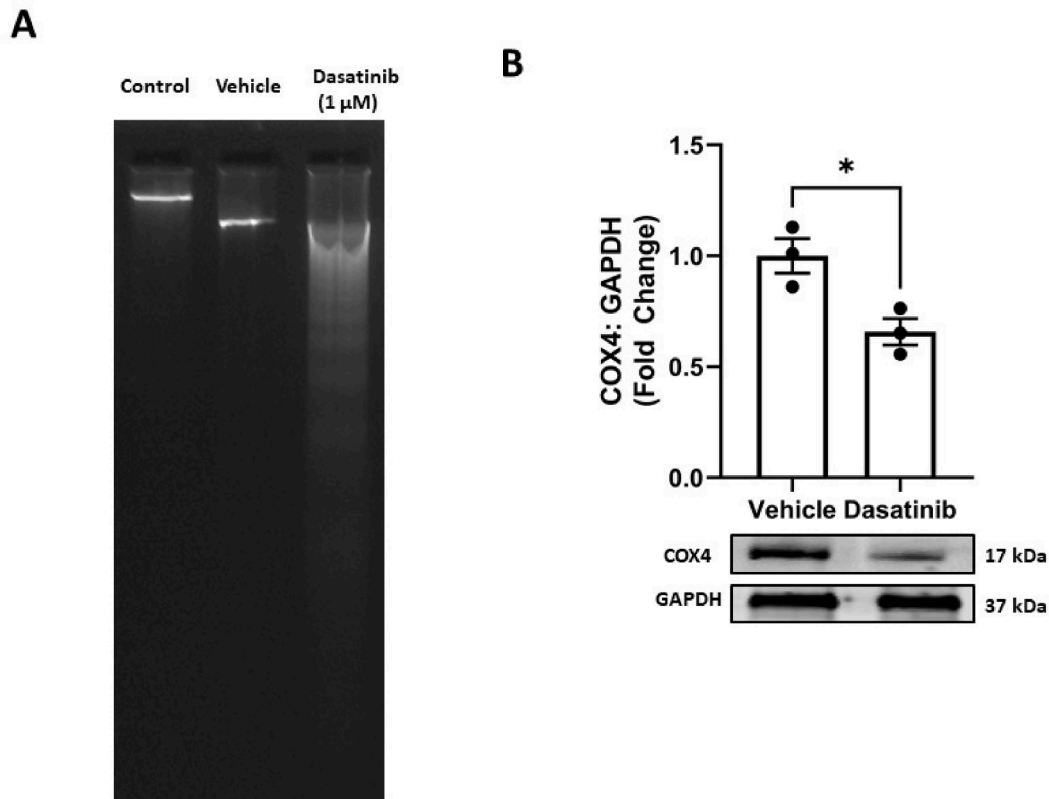
Fig. 1. Dasatinib induces mitochondrial damage in kidney cells. (A) Dasatinib (1 μM) induces fragmentation of mitochondrial DNA and (B) diminishes protein levels of mitochondrial-encoded subunit of respiratory chain complex IV (COX4) in human embryonic kidney 293 T cells. Briefly, 293 T cells were stressed using dasatinib (1 μM) for 6 h leading to mitochondrial damage. The mitochondrial DNA and total protein were collected, and DNA gels and immunoblots were performed according to the methods described in the sections above. The experiments were performed in a minimum of triplicates and significant differences were determined by one-way ANOVA followed by Dunnett's post-hoc test to compare means from peptide groups against the control group. *$p < 0.05$, **$p < 0.01$, ***$p < 0.001$ ****$p < 0.0001$.

increased the protein levels of SIRT3 ($p < 0.01$), a cytoprotective mitochondrial sirtuin, indicating mitochondrial protection against dasatinib stress. In line with these results, the protein levels of COX4, a vital biomarker for mitochondrial health, were significantly improved by GWN treatment (50 μM) ($p < 0.01$) (Fig. 3D). These results showed strong evidence of mitochondrial protection and rejuvenation by GWN and GW against dasatinib induced cellular injury.

3.4. Peptides GWN and GW increased antioxidant enzymes and lowered ROS

In line with the increased level of cytoprotective sirtuins (Fig. 3B,D), we observed a sharp decline in ROS levels induced by dasatinib injury by GWN and GW treatment ($p < 0.001$) (Fig. 4A). Ovotransferrin-derived peptides, GWN and GW, re-established redox homeostasis in cells by restoring the ROS levels to pre-injury levels (Fig. 4A). Levels of antioxidant enzyme, catalase, were significantly increased by GWN ($p < 0.001$) and GW ($p < 0.01$), confirming their protective role against oxidative stress (Fig. 4B,C). However, only GWN pre-treatment significantly increased ($p < 0.05$) the levels of SOD2 (superoxide dismutase 2) (Fig. 4C).

3.5. Mitochondrial protection extended by GWN and GW against dasatinib stress

Next, we conducted flow cytometry to evaluate the ability of GWN and GW to counter dasatinib induced mitochondrial loss (Fig. 5). Our results showed that compared to the vehicle, dasatinib (1 μM) caused a

significant decline in the mitochondrial density in kidney cells (Fig. 4A-B). This decline confirmed the previously observed mt.DNA damage and loss in COX4 levels following dasatinib injury in kidney cells (Fig. 1B). However, the pre-treatment of kidney cells with GWN and GW significantly abrogated the mitochondrial loss induced by dasatinib in kidney cells at the tested concentration (50 μM) (Fig. 5B-C). However, the ability of GWN to protect kidney cell mitochondria against dasatinib was stronger than GW (Fig. 5C-D). These results from flow cytometry analysis confirmed the ability of GWN and GW to attenuate kidney mitochondria loss and damage induced by dasatinib injury.

3.6. SIRT1 dependence of GWN and GW exhibited mitochondrial protection

Owing to the close relation of SIRT1 and renoprotection (Huang et al., 2020; Sun et al., 2021), and SIRT1 activation by GWN and GW, we inquired if the cytoprotective effects of these peptides were SIRT1 dependent. Our cell viability results showed that GWN and GW extended stronger protection against dasatinib injury in WT cells in comparison to SIRT1$^{-/-}$ cells ($p < 0.001$) (Fig. 6A). Likewise, the ability of GWN to increase COX4 (Fig. 3D) was diminished in SIRT1$^{-/-}$ cells (Fig. 6B). Similarly, there was a strong decline in the ability of GWN and GW to boost the H3K36me3 histone mark in SIRT1$^{-/-}$ cells (Fig. 6C) compared to WT cells (Fig. 2C). Overall, the loss of SIRT1 leads to abrogation of cytoprotection and epigenetic mechanisms exhibited by GWN and GW, indicating a SIRT1 dependent bioactivity of GWN and GW.
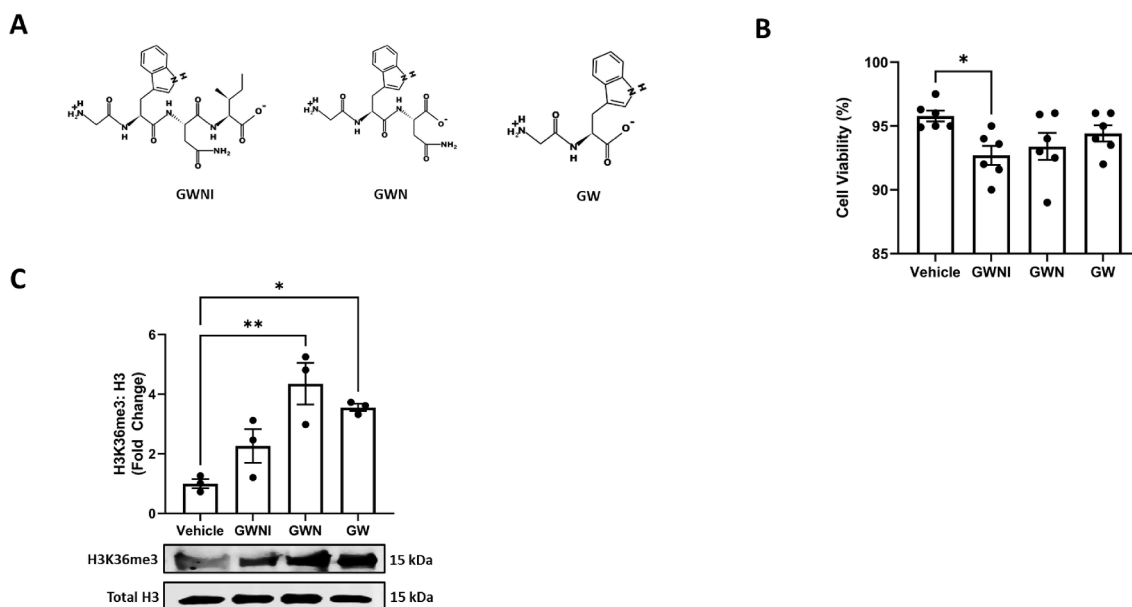
Fig. 2. Toxicity and histone modification ability of peptides originating from ovotransferrin. Two peptides, GWN and GW among (A) three antioxidant peptides induce (B) minimal toxicity in and (C) significantly improve active histone mark H3K36me3 in human embryonic kidney 293 T cells. Briefly, 293 T cells were treated with three peptides GWNI, GWN, and GW; and cell viability and histone extraction were performed. Cell viability was assessed using the trypan blue method on dual-chamber cell counting slides while histones were extracted using acid-based precipitation. The experiments were performed in a minimum of triplicates and significant differences were determined by one-way ANOVA followed by Dunnett's post-hoc test to compare means from peptide groups against the control group. *p < 0.05, **p < 0.01.
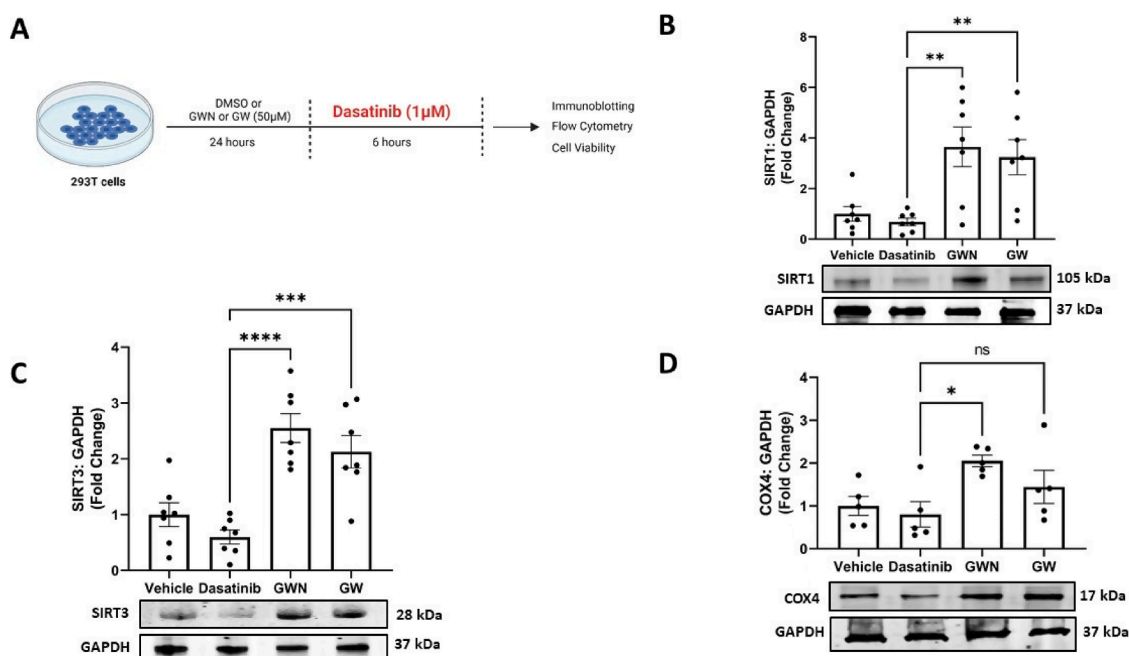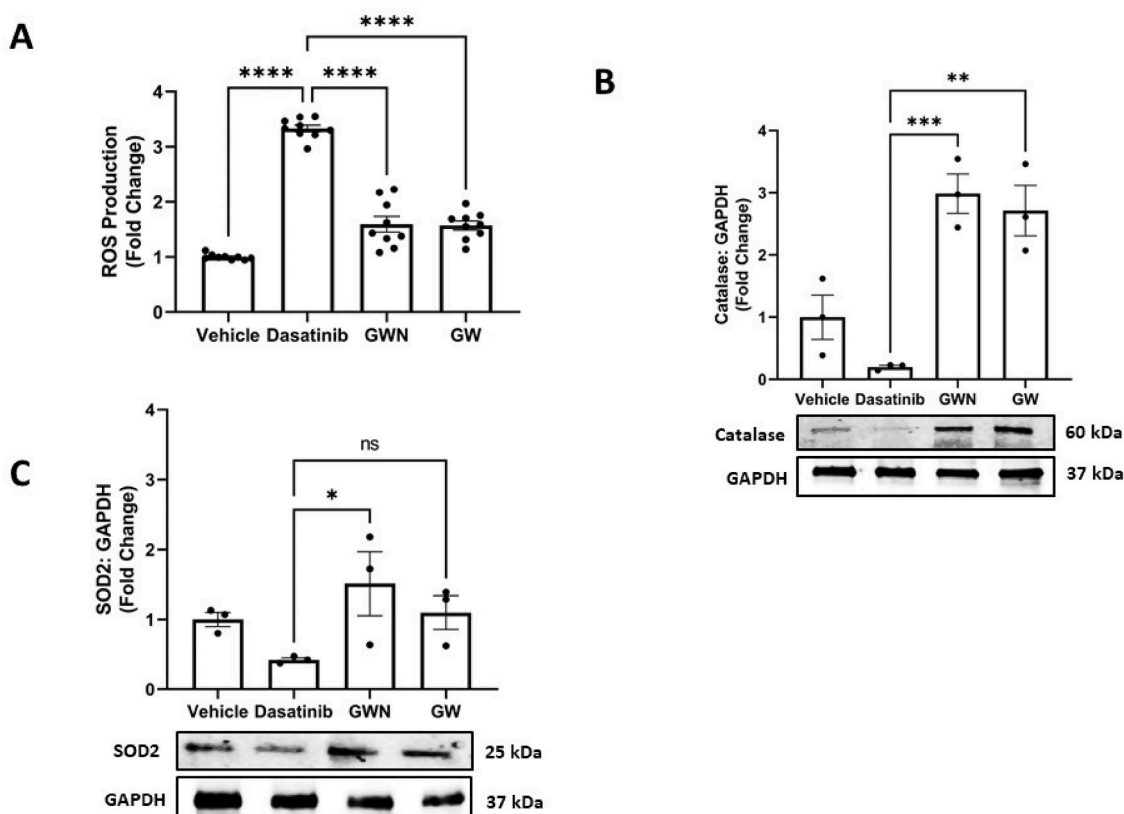

Fig. 3. Cytoprotection extended by peptides originating from ovotransferrin against Dasatinib injury in kidney cells. (A) Two peptides GWN, and GW increased (B) SIRT1 (C) SIRT3 (D) and COX4 levels following Dasatinib (1 μM) injury in human embryonic kidney 293 T cells. Briefly, 293 T cells were pre-treated with GWN and GW for 24 h, followed by cellular stress of dasatinib (1 μM) for 6 h. After these treatments, total protein was collected using RIPA buffer and immunoblots were performed. The experiments were performed in a minimum of triplicates and significant differences were determined by one-way ANOVA followed by Dunnett's post-hoc test to compare means from peptide groups against the control group. **p < 0.01.

3.7. Peptides GWN and GW exhibited potential bioavailability

Finally, we conducted a metabolism prediction study to forecast the metabolism and uptake of the two peptides. Our results showed that both peptides, GWN and GW, had very different properties as indicated

by the bioavailability radar (Fig. 7A,B). Polar surface area of GWN was higher compared to GW, as indicated by TPSA, considering sulfur and phosphorus as polar atoms (Fig. 7A,B). Next, the predictions for passive human gastrointestinal absorption (HIA) and blood–brain barrier (BBB) permeation shown in BOILED-Egg model, indicated higher absorption of

Fig. 4. Antioxidant activity extended by peptides originating from ovotransferrin against Dasatinib injury in kidney cells. Two peptides GWN, and GW (A) lowered ROS and increased (B) catalase and (C) SOD2 levels following Dasatinib (1 μM) injury in human embryonic kidney 293 T cells. Briefly, 293 T cells were pretreated with GWN and GW for 24 h, followed by cellular stress of dasatinib (1 μM) for 6 h. After these treatments, total protein was collected using RIPA buffer and immunoblots were performed. The experiments were performed in a minimum of triplicates and significant differences were determined by one-way ANOVA followed by Dunnett's post-hoc test to compare means from peptide groups against the control group. $**p < 0.01$.
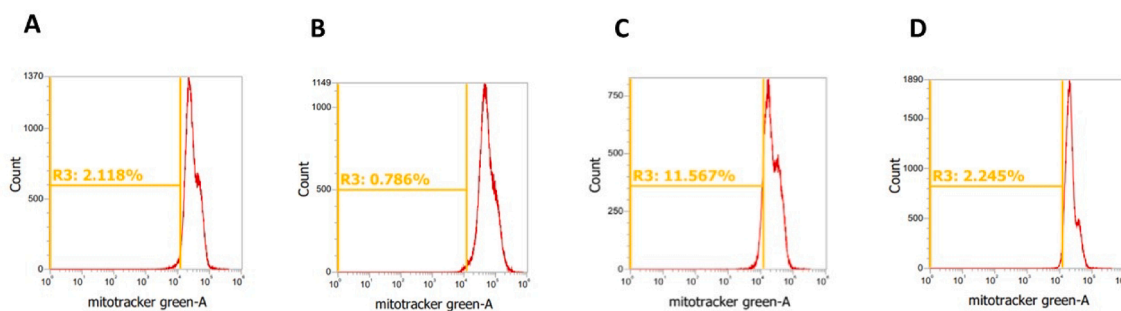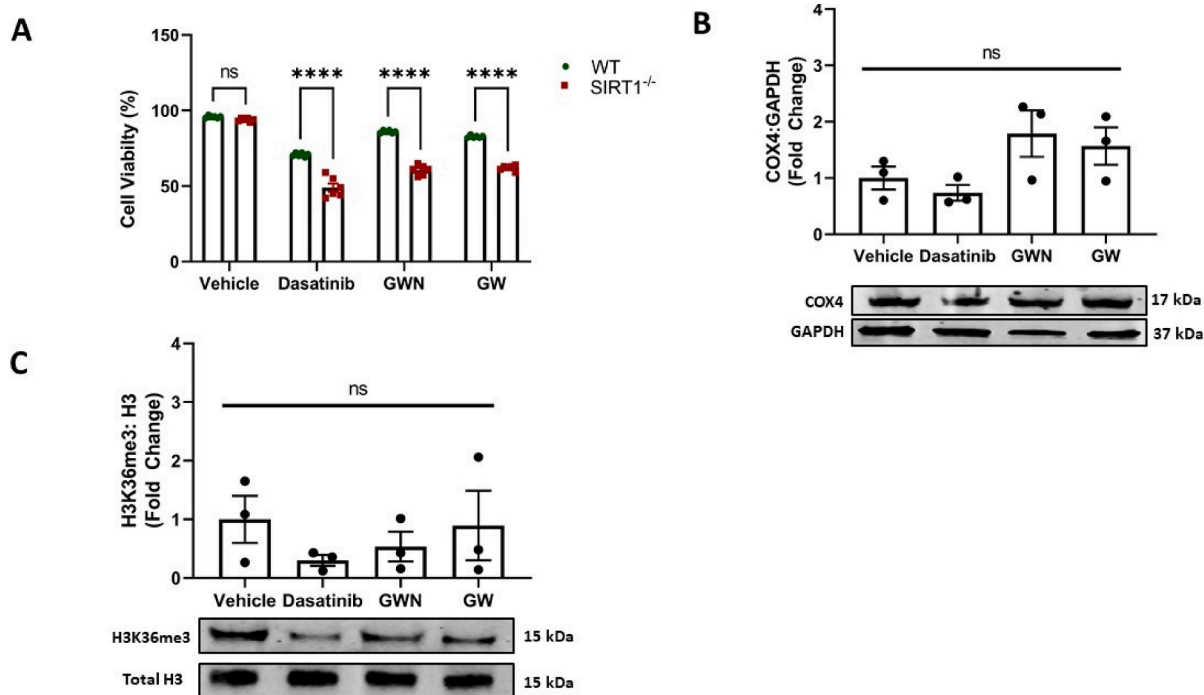

Fig. 5. Peptides originating from ovotransferrin protect mitochondria against Dasatinib injury in kidney cells. Compared to (A) vehicle, (B) dasatinib (1 μM) treatment leads to sharp decline in mitochondrial number which was recovered by and (C) GWN and (D) GW pool following injury in human embryonic kidney 293 T cells. Briefly, 293 T cells were pre-treated with GWN and GW for 24 h, followed by cellular stress of dasatinib (1 μM) for 6 h. After various treatments, cells were collected using trypsinization, incubated with MitoTracker™ Green FM at a 400 μM concentration and flow cytometry was conducted. The experiments were performed in a minimum of triplicate and analysis was conducted using the FlowJo software. (For interpretation of the references to colour in this figure legend, the reader is referred to the web version of this article.)

GW, compared to GWN peptide (Fig. 7C). However, the predicted bioavailability score of both peptides was equal (Fig. 7D), indicating ~ 55% bioavailability of 10% of fed peptides *in vivo*.
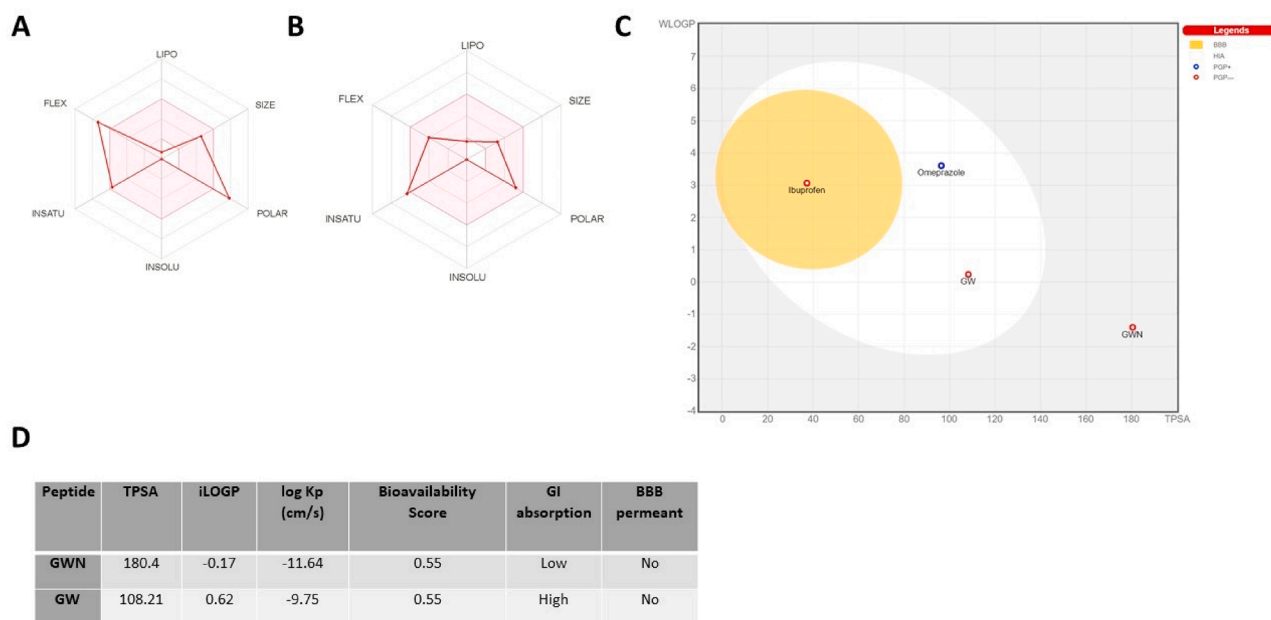
4. Discussion

Chemotherapy drugs have significantly enhanced the survival of cancer patients; however, these therapeutic agents are not without undesirable renal effects. Multiple studies have reported kidney injuries emerging from chemotherapy in>5 percent of cancer patients receiving standardized treatment (Kitchlu et al., 2019). Various chemotherapy agents have been coupled with kidney issues including glomerular disease, electrolyte imbalance, hypertension, and proteinuria (Glezerman & Jaimes, 2016). Dasatinib, a tyrosine kinase inhibitor, has been shown to inhibit many different tyrosine kinases and is primarily utilized in Imatinib-resistant chronic myeloid leukemia (CML) (Abbas, Mirza, Ganti, & Tendulkar, 2015). The mechanism by which dasatinib causes kidney injury is not fully understood, however, the role of mitochondrial stress and damage can't be ruled out (Toyama, Shimoyama, Szeto, Schiller, & Shimoyama, 2018). Herein, we identified GWN and GW, two

Fig. 6. SIRT1 dependence of cytoprotection extended by peptides originating from ovotransferrin against Dasatinib injury. Two peptides GWN, and GW maintain (A) cell viability (B) COX4 levels and (C) H3K36me3 levels following Dasatinib (1 μM) injury in a SIRT1 dependent manner in 293 T cells. Briefly, 293 T WT and 293 T SIRT1 KO cells were pre-treated with GWN and GW for 24 h, followed by cellular stress of dasatinib (1 μM) for 6 h. After treatments, cells were collected and cell viability, immunoblotting, and histone mark analysis were performed as described in the methods. The experiments were performed in a minimum of triplicates and significant differences were determined by one-way ANOVA followed by Dunnett's post-hoc test to compare means from peptide groups against the control group. $**p < 0.01$.

Peptide	TPSA	iLOGP	log Kp (cm/s)	Bioavailability Score	GI absorption	BBB permeant
GWN	180.4	-0.17	-11.64	0.55	Low	No
GW	108.21	0.62	-9.75	0.55	High	No

Fig. 7. Metabolic prediction of GWN and GW peptides originating from ovotransferrin. Graphics indicate (A-B) the bioavailability radars (C) the BOILED-Egg model of absorption and (D) key pharmacological properties of the two peptides. The canonical smiles of the two active peptides, GWN and GW, were generated using Open Babel software and processed using SwissADME along with appropriate control molecules. The program was run to obtain the BOILED-Egg results while the pharmacological data was obtained using CSV file provided by the software.

ovotransferrin derived antioxidant peptides as cytoprotective agents against dasatinib induced mitochondrial damage in kidney cells.

The physiological relevance of mitochondria is not only limited to

ATP production but extends to cellular metabolism, cell survival, and Ca^{2+} homeostasis (Spinelli et al., 2018). Kidneys consume ~ 10 percent of the body's oxygen to perform their functions, making them second

only to the heart in mitochondrial tally and oxygen consumption (Duann & Lin, 2017). Owing to the heavy reliance of kidneys on oxidative phosphorylation (OXPHOS) for tubular reabsorption, the role of mitochondrial homeostasis is critical to the preservation of normal kidney function (Soltoff, 1986). Hence, mitochondrial damage and dysfunction are now recognized as leading factors in various renal diseases. During the chemotherapy, kidneys are extremely susceptible to nephrotoxicity and mitochondrial damage due to their direct role in the metabolic processing and excretion of toxic agents (Perazella, 2009). This presents the renal mitochondrial dysfunction, a vital aspect of chemotherapy induced damage, as a target for alleviation of renal toxicity by cytoprotective agents, including bioactive peptides.

The prospect of complementing the kidney's antioxidant defense system with exogenous antioxidants in the form of antioxidant bioactive peptides is an attractive therapeutic approach. For instance, bioactive food peptides can serve directly or as food system ingredients for the prevention, and/or management of chemotherapy induced renal oxidative and mitochondrial damage. Firstly, our results show that the dasatinib triggered mitochondrial damage, as reflected by the mt.DNA breakage and loss of COX4 (Fig. 1 A,B). Next, in line with our proposed hypothesis, antioxidant peptides GWN and GW, with the ability to activate the H3K36me3 mark, attenuated this cellular damage in kidney cells. It is possible that the accrual of H3K36me3, a mark associated with actively transcribed genes, may act as the principal cytoprotective signal and reduce oxidative stress and mitochondrial damage in embryonic kidney cells (Hassan, Carlson, Abdallah, Buttolph, Glass, & Fandy, 2015). As H3K36 methylation promotes chromosome stability, increased accumulation of H3K36me3 levels by GWN and GW treatment may serve a defensive role in kidney cells from an evolutionary standpoint (Carrozza et al., 2005; Nicolas, Yamada, Cam, FitzGerald, Kobayashi, & Grewal, 2007). As histone modifications help to highlight exons from introns in various genes, therefore the possibility of amplified and specific transcription of cytoprotective genes cannot be ruled out. Also, the ability of the H3K36me3 histone mark to improve DNA repair and facilitate transcription elongation can be complementary factor(s) underlying the cytoprotective action of GWN and GW (Chen et al., 2015; Li et al., 2013). Likewise, both peptides managed to significantly lower cellular ROS induced by dasatinib injury in cells and boost antioxidant enzymes as well. We also predicted the GI absorption of both peptides, with stronger absorption of GW compared to GWN. Despite similar bioavailability score of 55%, higher predicted absorption of GW can be attributed to its lower TPSA values. As the negative impact of a high polar surface area on intestinal absorption is well recognized, supported by robust solvation free energy and *n*-octanol/water partition coefficient (iLOGP). This addresses the vital question of bioavailability and *in vivo* translation of the cellular findings. However, owing to the limited scope of this manuscript, an in-depth analysis of these cell signaling cascades was not conducted. Also, the activation of SIRT1, a *bona fide* histone deacetylase with the ability to shuttle cytoprotective signals between the nucleus and the mitochondria is a vital feature of GWN and GW.

Similar to our findings, the cytoprotective hormone erythropoietin protects against chemotherapy induced mitochondrial damage via SIRT1 dependent mechanisms (Cui et al., 2017). Another example includes use of erythropoietin and lunasin to treat chemotherapy induced kidney disease, anaemia, and immune dysfunction (Bennett et al., 2012; Chang et al., 2014). Likewise, a well-studied antioxidant tripeptide, IRW (Ile-Arg-Trp), also boosts NAMPT/NAD$^+$ levels in a SIRT1 dependent manner (Bhullar et al., 2021a). Also, it is important to note that activation of mitochondrially located SIRT3 by GWN can defend the mitochondrial DNA against oxidative damage (Cheng et al., 2013). A previous report has also shown that the activation of SIRT3 protects the mice heart from chemotherapy-induced mt.DNA damage (Pillai et al., 2016). Increased COX4 levels and sustained mitochondrial density in kidney cells following pre-treatment of GWN and GW confirm their ability to protect mitochondria against injury. Our findings are also in

accord with a role for lunasin, a 43 amino acid residue that protects liver cells against oxidative damage by a chemical oxidant (Fernández-Tomé, Ramos, Cordero-Herrera, Recio, Goya, & Hernández-Ledesma, 2014). Mitochondrial peptide humanin also protects against chemotherapy induced bone growth impairment *in vivo* (Eriksson et al., 2014). Szeto–Schiller (SS) peptide-20, a mitochondria-targeted peptide protects against the development of oxaliplatin-induced neurological complications (Toyama et al., 2018). Similarly, α-melanocyte-stimulating peptide, protects against chemotherapy-induced alopecia in a clinical study (Böhm, Bodo, Funk, & Paus, 2014). Both GWN and GW exhibited kidney cell protection similar to SS-20 and SS-31, a mitochondria-targeted peptide with strong antioxidant activity (Liu et al., 2019; Sweetwyne et al., 2017; Toyama et al., 2018). Further, food derived bioactive peptides from kefir fermented milk protein and potatoes have shown the ability to protect kidneys from oxidative and mitochondrial damage (Chen et al., 2020; Tsai et al., 2020). Similarly, bioactive such as xanthones and polyphenols (such as ellagic acid) also exhibit kidney protective effects against mitochondrial oxidative damage (Aslan, Gok, Beyaz, Ağca, Erman, & Zerek, 2020; Rana, Tangpong, & Rahman, 2020). Isoliquiritigenin, a potent antioxidant polyphenol protects against chemotherapy-induced kidney and mitochondrial damage (Lee, Son, Park, Park, Lim, & Chung, 2008). Despite the numerous studies addressing the antioxidant and cytoprotective role of bioactive peptides, only a few research findings have been reported about the protective function in kidneys against chemotherapy. However, future studies, particularly focusing on animal models of chemotherapy-induced renal damage are required to assess *in vivo* translation of these cell results. These studies will also help shed light on *in vivo* toxicology, bioavailability, immune tolerance, and the long-term efficacy/applicability of these peptides. Overall, animal model studies can further support the exploration of bioactive peptides as cytoprotective agents against chemotherapy drugs that induced nephrotoxicity and mitochondrial damage.

5. Conclusions

In this study, we reported GWN and GW as cytoprotective antioxidant peptides with the ability to protect embryonic kidney cells against dasatinib induced mitochondrial damage. These peptides exhibited the ability to activate H3K36me3, a cytoprotective histone mark, along with SIRT1 and SIRT3. Both peptides recovered dasatinib induced mitochondrial damage as evidenced by an increase in COX4, antioxidant enzymes, lower ROS, and sustained mitochondrial density in kidney cells. Taken together, our findings support a potential role for bioactive peptides as cytoprotective agents against chemotherapy-induced mitochondrial damage and kidney toxicity. Further studies on the in-depth mechanisms along with animal studies will contribute to a better understanding of cellular processes involved in renal protection extended by the investigated peptides.

CRediT authorship contribution statement

Khushwant S. Bhullar: Conceptualization, Investigation, Data curation. **Fatemeh Ashkar:** Investigation. **Jianping Wu:** Conceptualization, Project administration, Resources, Supervision.

Declaration of Competing Interest

The authors declare that they have no known competing financial interests or personal relationships that could have appeared to influence the work reported in this paper.

References

Abbas, A., Mirza, M. M., Ganti, A. K., & Tendulkar, K. (2015). Renal toxicities of targeted therapies. *Targeted Oncology, 10*(4), 487–499.

Aslan, A., Gok, O., Beyaz, S., Ağca, C. A., Erman, O., & Zerek, A. (2020). Ellagic acid prevents kidney injury and oxidative damage via regulation of Nrf-2/NF-κB signaling in carbon tetrachloride induced rats. *Molecular Biology Reports, 47*(10), 7959–7970.

Balat, A., Resic, H., Bellinghieri, G., & Anarat, A. (2012). Devil's Triangle in Kidney Diseases: Oxidative Stress, Mediators, and Inflammation. Hindawi.

Bennett, C.L., Spiegel, D.M., Macdougall, I.C., Norris, L., Qureshi, Z.P., Sartor, O., Lai, S. Y., Tallman, M.S., Raisch, D.W., Smith, S.W. & Silver, S. (2012). A review of safety, efficacy, and utilization of erythropoietin, darbepoetin, and peginesatide for patients with cancer or chronic kidney disease: a report from the Southern Network on Adverse Reactions (SONAR). *In Seminars in thrombosis and hemostasis 38*(8), 783-796.

Bhullar, K. S., Son, M., Kerek, E., Cromwell, C. R., Wingert, B. M., Wu, K., … Wu, J. (2021a). Tripeptide IRW Upregulates NAMPT Protein Levels in Cells and Obese C57BL/6J Mice. *Journal of Agricultural and Food Chemistry*.

Bhullar, K. S., Son, M., Kerek, E., Cromwell, C. R., Wingert, B. M., Wu, K., … Wu, J. (2021b). Tripeptide IRW Upregulates NAMPT Protein Levels in Cells and Obese C57BL/6J Mice. *Journal of Agricultural and Food Chemistry, 69*(5), 1555–1566.

Bhullar, K. S., & Wu, J. (2020). Dietary peptides in aging: Evidence and prospects. *Food Science and Human Wellness, 9*(1), 1–7.

Boccellino, M., Cuccovillo, F., Napolitano, M., Sannolo, N., Balestrieri, C., Acampora, A., … Quagliuolo, L. (2003). Styrene-7, 8-oxide activates a complex apoptotic response in neuronal PC12 cell line. *Carcinogenesis, 24*(3), 535–540.

Böhm, M., Bodo, E., Funk, W., & Paus, R. (2014). α-Melanocyte-stimulating hormone: A protective peptide against chemotherapy-induced hair follicle damage? *British Journal of Dermatology, 170*(4), 956–960.

Bouitbir, J., Panajatovic, M. V., Frechard, T., Roos, N. J., & Krähenbühl, S. (2020). Imatinib and dasatinib provoke mitochondrial dysfunction leading to oxidative stress in C2C12 myotubes and human RD cells. *Frontiers in Pharmacology, 11*, 1106.

Burke, P. J. (2017). Mitochondria, bioenergetics and apoptosis in cancer. *Trends in Cancer, 3*(12), 857–870.

Carrozza, M. J., Li, B., Florens, L., Suganuma, T., Swanson, S. K., Lee, K. K., … Washburn, M. P. (2005). Histone H3 methylation by Set2 directs deacetylation of coding regions by Rpd3S to suppress spurious intragenic transcription. *Cell, 123*(4), 581–592.

Cermakova, K., Smith, E. A., Veverka, V., & Hodges, H. C. (2019). Dynamics of transcription-dependent H3K36me3 marking by the SETD2: IWS1: SPT6 ternary complex. *bioRxiv*, Article 636084.

Chang, H. C., Lewis, D., Tung, C. Y., Han, L., Henriquez, S. M., Voiles, L., Lupov, I. P., Pelloso, D., Sinn, A. L., Pollok, K. E., & Ben, O. (2014). Soypeptide lunasin in cytokine immunotherapy for lymphoma. *Cancer Immunology, Immunotherapy, 63*(3), 283–295.

Chen, K., Chen, Z., Wu, D., Zhang, L., Lin, X., Su, J., … Chen, X. (2015). Broad H3K4me3 is associated with increased transcription elongation and enhancer activity at tumor-suppressor genes. *Nature Genetics, 47*(10), 1149–1157.

Chen, Y.-H., Chen, H.-L., Fan, H.-C., Tung, Y.-T., Kuo, C.-W., Tu, M.-Y., & Chen, C.-M. (2020). Anti-inflammatory, antioxidant, and antifibrotic effects of kefir peptides on salt-induced renal vascular damage and dysfunction in aged stroke-prone spontaneously hypertensive rats. *Antioxidants, 9*(9), 790.

Cheng, Y., Ren, X., Gowda, A. S., Shan, Y., Zhang, L., Yuan, Y., . . . Yang, J. (2013). Interaction of Sirt3 with OGG1 contributes to repair of mitochondrial DNA and protects from apoptotic cell death under oxidative stress. Cell Death & Disease, 4(7), e731-e731.

Cui, L., Guo, J., Zhang, Q., Yin, J., Li, J., Zhou, W., … Zhang, L. (2017). Erythropoietin activates SIRT1 to protect human cardiomyocytes against doxorubicin-induced mitochondrial dysfunction and toxicity. *Toxicology Letters, 275*, 28–38.

DiFiore, J. V., Ptacek, T. S., Wang, Y., Li, B., Simon, J. M., & Strahl, B. D. (2020). Unique and shared roles for histone H3K36 methylation states in transcription regulation functions. *Cell Reports, 31*(10), Article 107751.

Duann, P., & Lin, P.-H. (2017). Mitochondria damage and kidney disease. *Mitochondrial Dynamics in Cardiovascular Medicine*, 529–551.

Eriksson, E., Wickström, M., Perup, L. S., Johnsen, J. I., Eksborg, S., Kogner, P., & Sävendahl, L. (2014). Protective role of humanin on bortezomib-induced bone growth impairment in anticancer treatment. *Journal of the National Cancer Institute, 106*(3), djt459.

Fan, H., Bhullar, K. S., & Wu, J. (2021). Spent Hen Muscle Protein-Derived RAS Regulating Peptides Show Antioxidant Activity in Vascular Cells. *Antioxidants, 10*(2), 290.

Fernández-Tomé, S., Ramos, S., Cordero-Herrera, I., Recio, I., Goya, L., & Hernández-Ledesma, B. (2014). In vitro chemo-protective effect of bioactive peptide lunasin against oxidative stress in human HepG2 cells. *Food Research International, 62*, 793–800.

Glezerman, I. G., & Jaimes, E. A. (2016). Chemotherapy and kidney injury. *American Society of Nephrology*, 1–10.

Guignabert, C., Phan, C., Seferian, A., Huertas, A., Tu, L., Thuillet, R., … Jutant, E.-M. (2016). Dasatinib induces lung vascular toxicity and predisposes to pulmonary hypertension. *The Journal of Clinical Investigation, 126*(9), 3207–3218.

Hassan, H. E., Carlson, S., Abdallah, I., Buttolph, T., Glass, K. C., & Fandy, T. E. (2015). Curcumin and dimethoxycurcumin induced epigenetic changes in leukemia cells. *Pharmaceutical Research, 32*(3), 863–875.

Hoenig, M. P., & Zeidel, M. L. (2014). Homeostasis, the milieu interieur, and the wisdom of the nephron. *Clinical Journal of the American Society of Nephrology, 9*(7), 1272–1281.

Holstein, S. A., Stokes, J. B., & Hohl, R. J. (2009). Renal failure and recovery associated with second-generation Bcr-Abl kinase inhibitors in imatinib-resistant chronic myelogenous leukemia. *Leukemia Research, 33*(2), 344–347.

Huang, X., Shi, Y., Chen, H., Le, R., Gong, X., Xu, K., … Gu, X. (2020). Isoliquiritigenin prevents hyperglycemia-induced renal injuries by inhibiting inflammation and oxidative stress via SIRT1-dependent mechanism. *Cell Death & Disease, 11*(12), 1–14.

Jahandideh, F., Chakrabarti, S., Davidge, S. T., & Wu, J. (2016). Antioxidant peptides identified from ovotransferrin by the ORAC method did not show anti-inflammatory and antioxidant activities in endothelial cells. *Journal of Agricultural and Food Chemistry, 64*(1), 113–119.

Kitchlu, A., McArthur, E., Amir, E., Booth, C. M., Sutradhar, R., Majeed, H., … Chan, C. T. (2019). Acute kidney injury in patients receiving systemic treatment for cancer: A population-based cohort study. *JNCI: Journal of the National Cancer Institute, 111*(7), 727–736.

Kluge, M. A., Fetterman, J. L., & Vita, J. A. (2013). Mitochondria and endothelial function. *Circulation Research, 112*(8), 1171–1188.

Krata, N., Zagożdżon, R., Foroncewicz, B., & Mucha, K. (2018). Oxidative stress in kidney diseases: The cause or the consequence? *Archivum immunologiae et therapiae experimentalis, 66*(3), 211–220.

Lee, C. K., Son, S. H., Park, K. K., Park, J. H. Y., Lim, S. S., & Chung, W. Y. (2008). Isoliquiritigenin inhibits tumor growth and protects the kidney and liver against chemotherapy-induced toxicity in a mouse xenograft model of colon carcinoma. *Journal of Pharmacological Sciences, 106*(3), 444–451.

Lee, J. H., Moon, S. H., Kim, H. S., Park, E., Ahn, D. U., & Paik, H. D. (2017). Antioxidant and anticancer effects of functional peptides from ovotransferrin hydrolysates. *Journal of the Science of Food and Agriculture, 97*(14), 4857–4864.

Li, F., Mao, G., Tong, D., Huang, J., Gu, L., Yang, W., & Li, G.-M. (2013). The histone mark H3K36me3 regulates human DNA mismatch repair through its interaction with MutSα. *Cell, 153*(3), 590–600.

Li, T., Garcia-Gomez, A., Morante-Palacios, O., Ciudad, L., Özkaramehmet, S., Van Dijck, E., … Ballestar, E. (2020). SIRT1/2 orchestrate acquisition of DNA methylation and loss of histone H3 activating marks to prevent premature activation of inflammatory genes in macrophages. *Nucleic Acids Research, 48*(2), 665–681.

Liu, D., Jin, F., Shu, G., Xu, X., Qi, J., Kang, X., … Han, F. (2019). Enhanced efficiency of mitochondria-targeted peptide SS-31 for acute kidney injury by pH-responsive and AKI-kidney targeted nanopolyplexes. *Biomaterials, 211*, 57–67.

Maher, H. M., Alzoman, N. Z., Shehata, S. M., & Abanmy, N. O. (2018). Validated UPLC-MS/MS method for the quantification of dasatinib in plasma: Application to pharmacokinetic interaction studies with nutraceuticals in Wistar rats. *PloS One, 13*(6), Article e0199208.

Martijn, J., Vosseberg, J., Guy, L., Offre, P., & Ettema, T. J. (2018). Deep mitochondrial origin outside the sampled alphaproteobacteria. *Nature, 557*(7703), 101–105.

Nicolas, E., Yamada, T., Cam, H. P., FitzGerald, P. C., Kobayashi, R., & Grewal, S. I. (2007). Distinct roles of HDAC complexes in promoter silencing, antisense suppression and DNA damage protection. *Nature Structural & Molecular Biology, 14*(5), 372–380.

Ozkurt, S., Temiz, G., Acikalin, M. F., & Soydan, M. (2010). Acute renal failure under dasatinib therapy. *Renal Failure, 32*(1), 147–149.

Perazella, M. A. (2009). Renal vulnerability to drug toxicity. *Clinical Journal of the American Society of Nephrology, 4*(7), 1275–1283.

Pillai, V. B., Bindu, S., Sharp, W., Fang, Y. H., Kim, G., Gupta, M., … Gupta, M. P. (2016). Sirt3 protects mitochondrial DNA damage and blocks the development of doxorubicin-induced cardiomyopathy in mice. *American Journal of Physiology-Heart and Circulatory Physiology, 310*(8), H962–H972.

Piscitani, L., Sirolli, V., Di Liberato, L., Morroni, M., & Bonomini, M. (2020). Nephrotoxicity Associated with Novel Anticancer Agents (Aflibercept, Dasatinib, Nivolumab): Case Series and Nephrological Considerations. *International Journal of Molecular Sciences, 21*(14), 4878.

Rana, M. N., Tangpong, J., & Rahman, M. A. (2020). Xanthones protects lead-induced chronic kidney disease (CKD) via activating Nrf-2 and modulating NF-kB, MAPK pathway. *Biochemistry and Biophysics Reports, 21*, Article 100718.

Sena, C. M., Pereira, A. M., & Seiça, R. (2013). Endothelial dysfunction—a major mediator of diabetic vascular disease. *Biochimica et Biophysica Acta (BBA)-Molecular Basis of Disease, 1832*(12), 2216–2231.

Shang, N., Bhullar, K. S., & Wu, J. (2020). Ovotransferrin Exhibits Osteogenic Activity Partially via Low-Density Lipoprotein Receptor-Related Protein 1 (LRP1) Activation in MC3T3-E1 Cells. *Journal of Agricultural and Food Chemistry, 68*(35), 9427–9435.

Shechter, D., Dormann, H. L., Allis, C. D., & Hake, S. B. (2007). Extraction, purification and analysis of histones. *Nature Protocols, 2*(6), 1445.

Shen, S., Chahal, B., Majumder, K., You, S.-J., & Wu, J. (2010). Identification of novel antioxidative peptides derived from a thermolytic hydrolysate of ovotransferrin by LC-MS/MS. *Journal of Agricultural and Food Chemistry, 58*(13), 7664–7672.

Sims Iii, R. J., & Reinberg, D. (2009). Processing the H3K36me3 signature. *Nature Genetics, 41*(3), 270–271.

Soltoff, S. P. (1986). ATP and the regulation of renal cell function. *Annual Review of Physiology, 48*(1), 9–31.

Spinelli, J. B., & Haigis, M. C. (2018). The multifaceted contributions of mitochondria to cellular metabolism. *Nature Cell Biology, 20*(7), 745–754.

Sun, H.-J., Xiong, S.-P., Cao, X., Cao, L., Zhu, M.-Y., Wu, Z.-Y., & Bian, J.-S. (2021). Polysulfide-mediated sulfhydration of sirt1 prevents diabetic nephropathy by

suppressing phosphorylation and acetylation of p65 nf-κb and stat3. *Redox Biology, 38,* Article 101813.

Sun, Z., Zhang, Y., Jia, J., Fang, Y., Tang, Y., Wu, H., & Fang, D. (2020). H3K36me3, message from chromatin to DNA damage repair. *Cell & Bioscience, 10*(1), 1–9.

Sweetwyne, M. T., Pippin, J. W., Eng, D. G., Hudkins, K. L., Chiao, Y. A., Campbell, M. D., … Rabinovitch, P. S. (2017). The mitochondrial-targeted peptide, SS-31, improves glomerular architecture in mice of advanced age. *Kidney International, 91*(5), 1126–1145.

Toyama, S., Shimoyama, N., Szeto, H. H., Schiller, P. W., & Shimoyama, M. (2018). Protective effect of a mitochondria-targeted peptide against the development of chemotherapy-induced peripheral neuropathy in mice. *ACS Chemical Neuroscience, 9* (7), 1566–1571.

Tryfonopoulos, D., O'Donovan, N., Corkery, B., Clynes, M., & Crown, J. (2009). Activity of dasatinib with chemotherapy in triple-negative breast cancer cells. Journal of Clinical Oncology, *27*(15_suppl), e14605-e14605.

Tsai, B.-C.-K., Hsieh, D.-J.-Y., Lin, W.-T., Tamilselvi, S., Day, C. H., Ho, T.-J., … Huang, C.-Y. (2020). Functional potato bioactive peptide intensifies Nrf2-dependent

antioxidant defense against renal damage in hypertensive rats. *Food Research International, 129,* Article 108862.

Tu, S., Bulloch, E. M., Yang, L., Ren, C., Huang, W.-C., Hsu, P.-H., … Lo, W.-S. (2007). Identification of histone demethylases in Saccharomyces cerevisiae. *Journal of Biological Chemistry, 282*(19), 14262–14271.

Wallace, E., Lyndon, W., Chumley, P., Jaimes, E. A., & Fatima, H. (2013). Dasatinib-induced nephrotic-range proteinuria. *American Journal of Kidney Diseases, 61*(6), 1026–1031.

Will, Y., Dykens, J. A., Nadanaciva, S., Hirakawa, B., Jamieson, J., Marroquin, L. D., … Jessen, B. A. (2008). Effect of the multitargeted tyrosine kinase inhibitors imatinib, dasatinib, sunitinib, and sorafenib on mitochondrial function in isolated rat heart mitochondria and H9c2 cells. *Toxicological Sciences, 106*(1), 153–161.

Wu, Y., Wang, Y., & Nabi, X. (2019). Protective effect of Ziziphora clinopodioides flavonoids against H2O2-induced oxidative stress in HUVEC cells. *Biomedicine & Pharmacotherapy, 117,* Article 109156.

Xue, T., Luo, P., Zhu, H., Zhao, Y., Wu, H., Gai, R., … He, Q. (2012). Oxidative stress is involved in Dasatinib-induced apoptosis in rat primary hepatocytes. *Toxicology and Applied Pharmacology, 261*(3), 280–291.